LAWRENCE
LIVERMORE
NATIONAL
LABORATORY

UCRL-JRNL-203988

High-speed horizontal-path atmospheric turbulence correction using a large actuator-number MEMS spatial light modulator in an interferometric phase conjugation engine

Kevin Baker, Eddy Stappaerts, Don Gavel, Scott Wilks, Jack Tucker, Dennis Silva, Jeff Olsen, Scot Olivier, Peter Young, Mike Kartz, Laurence Flath, Peter Kruelivitch, Jackie Crawford, Oscar Azucena

May 5, 2004

Optics Letters

High-speed horizontal-path atmospheric turbulence correction using a large actuator-number MEMS spatial light modulator in an interferometric phase conjugation engine

K.L. Baker, E.A. Stappaerts, D. Gavel, S.C. Wilks, J. Tucker, D.A. Silva, J. Olsen, S.S. Olivier, P.E. Young, M.W. Kartz, L.M. Flath, P. Kruelevitch, J. Crawford and Oscar Azucena

Lawrence Livermore National Laboratory, Livermore, CA, USA

Abstract

Atmospheric propagation results for a high-speed, large-actuator-number, adaptive optics system are presented. The system uses a MEMS-based spatial light modulator correction device with 1024 actuators. Tests over a 1.35 km path achieved correction speeds in excess of 800 Hz and Strehl ratios close to 0.5. The wave-front sensor was based on a quadrature interferometer that directly measures phase. This technique does not require global wave-front reconstruction, making it relatively insensitive to scintillation and phase residues. The results demonstrate the potential of large actuator number MEMS-based spatial light modulators to replace conventional deformable mirrors.

OCIS codes: 010.1080, 010.7350, 120.2880, 090.1000

Adaptive optics (AO) systems used in astronomy and vision applications typically utilize Shack-Hartmann wave-front sensors.[1,2] Shack-Hartmann wave-front sensors have also been employed for horizontal and slant path free space communications systems.[3] These sensors measure the gradient of the phase and commonly utilize least squares phase reconstruction algorithms. When coherent light propagates over atmospheric paths, the beam develops large intensity fluctuations and phase residues,[4] severely degrading the performance of these wave-front sensors. Interferometers, which measure phase directly, have been implemented in AO systems,[5,6] however, these systems are required to run in closed-loop to achieve a high Strehl ratio since they only sense one interferogram and, therefore, can only uniquely assign a phase value from 0 to π radians. Closed-loop in this context means that the correction applied to the spatial-light-modulator in the previous pass through the loop is sensed by the interferometer.

Recently, a prototype of the coherent light AO system described in this article was demonstrated using a visible laser and a liquid crystal spatial light modulator (SLM).[7] It allowed many concept features to be tested, but its speed was limited to ~1 Hz due to the SLM response time. This article discusses a coherent light AO system based on a quadrature Twyman-Green interferometer operating at a wavelength of 1.5 μm and at speeds in excess of 800 Hz through atmospheric turbulence. The system uses a 1024 actuator MEMS-based spatial light modulator, which represents an approximate order of magnitude increase in the number of actuators from previous MEMS-based SLMs used in AO systems.[3,8] The technique mixes an atmospheric probe beam with a large amplitude reference beam, allowing it operate in a photon-noise limited regime even in case of large scintillation. It does not require a global reconstruction of the phase, making it much less

sensitive to phase residues.[9] These attributes make this approach to phase conjugation much more robust than conventional AO systems employing shack-Hartmann wave-front sensors, for applications involving coherent light propagation through strong turbulence. Other approaches to horizontal path correction using adaptive optics include methods based on the stochastic parallel gradient descent algorithm[10] and curvature sensors.

An optical layout is shown in Fig. 1. The system consists primarily of an interferometric wave-front sensor, a MEMS-based SLM built by the Boston Micromachines Corporation (BMC),[11] a 1.5 μm Erbium-doped fiber laser built by HRL Laboratories and computer hardware/software to analyze the wave-front and implement the phase correction. The system was designed for open-loop operation, however, a closed-loop arm exists to align the wave-front camera precisely with the SLM and either configuration can be used simply by blocking the remaining beam path. Alignment of the wave-front camera to the SLM is accomplished by writing phase patterns onto the SLM, determining the resulting phase on the wave-front camera and performing a cross-correlation between the measured phase pattern and the pattern written to the SLM to determine the offset between the two. The laser has two independently triggerable arms that produce nearly transform-limited pulses of 1 ns duration and energies of 7 μJ and 100 nJ for the probe beam and the reference beam, respectively.

The topology of the field test site was defined by rolling hills. The experiment was carried out across a valley between two of these hills, one of which contained the AO system and the other a 2-mirror retro-reflector. The AO system was slightly higher in elevation than the retro-reflector, with an approximate drop in elevation of 100 meters to

the valley floor between the two hills. The roundtrip distance traveled by the probe beam was approximately 1.35 km, for a transit time of approximately 4.5 μs.

The turbulence over the propagation path was characterized by measuring the aberrated phase profile of the probe beam after passing through the atmosphere. A large number of interferograms, ~3000, were acquired at a frequency of ~580 Hz. These interferograms contained the information required to determine the two-dimensional, wrapped (modulo-2π), phase across the input aperture of the system. Before the parameters used to describe the turbulence spectrum could be determined, the phase was unwrapped using a minimum weighted discontinuity method.[12] This technique partitions the wrapped phase profile into two connected regions separated by discontinuity curves. The algorithm then raises the phase in one of the regions by 2π, thereby reducing the weighted sum of the discontinuities. This process is repeated until no further partitioning is possible. One important scaling relation is the phase structure function, $D_\phi(r)$, defined by $D_\phi(r) = \langle | \phi(x) - \phi(x+r)|^2 \rangle$. For a Kolmogorov turbulence spectrum the phase structure function can be expressed analytically as $D_\phi(r) = 6.88(r/r_o)^{5/3}$. In this expression r_0 is the Fried parameter, also known as the transverse coherence length. The phase structure function is constructed by comparing the phase at a given location to the phase at an increasing distance from that location. An average over 3000 such functions is shown in Fig. 2. There is a good fit between the slopes of the averaged, experimentally determined, function and the analytic form for a Kolmogorov turbulence spectrum. The solid black line represents the data, the solid gray line represents the Kolmogorov fit for a Fried parameter of 2.4 cm and the two dashed black lines represent Kolmogorov fits for Fried parameters of 2.0 cm and 3.0 cm, respectively. The constant of 6.88 in the analytic

expression above is valid for $r >> (\lambda L)^{0.5}$ and approaches the value 3.44 when $r << (\lambda L)^{0.5}$, where λ is the probe wavelength and L is the propagation length.[13] The fit of the data to the analytic expression occurred over a range where $r \sim (\lambda L)^{0.5}$; however, using the value of 6.88 should result in an overestimate of r_o of less than 20 %.

The performance of the AO system was quantified by measuring the Strehl ratio. The Strehl ratio was calculated by measuring both the point-spread function (PSF), with a far-field camera, and the near-field image of the probe beam, with the wave-front camera. The near field images were collected at a slightly delayed time by blocking the reference beam. Fig. 3 shows the PSF for the uncorrected probe beam, Fig. 3a, and the corrected probe beam, Fig. 3b. With these two measurements, the Strehl ratio was calculated and compared with the expected phase variance associated with a Kolmogorov turbulence spectrum. A sequence of 100 PSFs was taken and the absolute instantaneous Strehl ratios determined from these measurements, with the system on and off, as shown in Fig. 4. The instantaneous Strehl ratios were averaged over the 100 frames to quantify the system performance. The figure indicates a corrected Strehl ratio of S_r=0.46, a tip/tilt only Strehl ratio of S_r=0.19 and a Strehl ratio of S_r=0.06 without tip/tilt correction. The uncorrected value, S_r=0.06, is in reasonably good agreement with the expected value of $S_r=(r_o/D)^2=(2.4 \text{ cm}/13 \text{ cm})^2=0.03$.

An estimate of the Strehl ratio with the system on was made as follows. The ratio due to the fitting error, for a Kolmogorov turbulence spectrum and a square aperture, is given by $S_r=\exp\{-1.3(d/r_o)^{5/3}\}$, where d is the sub-aperture size. For the field test, the sub-aperture size was approximately 4 mm, yielding an expected Strehl ratio of Sr ~ 0.94. The SLM had approximately 60 bad pixels and the outer actuators were not activated,

such that 18% of the actuators were not contributing to the correction. Simulations performed taking these bad pixels into account indicated a reduction in the Strehl ratio of approximately 22%, giving an estimated maximum achievable Strehl ratio of S_r=(1.0-0.22)exp{-1.3$(d/r_o)^{5/3}$}~0.73. Given the wind velocities and system operating speeds, the effects of time delay error were negligible. The achievable Strehl ratio is further reduced by the 3-bit algorithm used to determine the phase, lowering it by a factor of 0.95 to S_r~0.95*0.73 = 0.69.[9,14] The measured value of 0.46 is then within approximately 40 % of the maximum achievable Strehl ratio. The discrepancy is likely due to slight registration errors, camera gain nonlinearities and small errors in calibration of the SLM response curves.

In the field test, the AO system achieved large improvements, ~8x, over the uncorrected PSF. The system successfully demonstrated the use of a large actuator number, 1024, MEMS-based SLM at speeds in excess of 800 Hz. This work demonstrates the potential of such SLMs to replace conventional deformable mirrors for applications requiring high Strehl ratios such as multi-conjugate and extreme AO systems, AO systems for extremely large telescopes and communications and imaging under conditions of strong turbulence.

The authors would like to acknowledge M.L. Minden, Hughes Research Laboratories, for providing the Erbium-doped fiber laser and P. Bierden, Boston MicroMachines Corporation, for providing the MEMS-based spatial light modulator. The authors would also like to acknowledge discussions with W.H Long, Jr (NGST) regarding simulations, H. Komine (NGST) for suggesting a Wollaston prism in the configuration shown in Fig. 1 and L.G. Seppala (LLNL) for contributions to the optical

design. This work was performed as part of the Coherent Communications, Imaging and Targeting (CCIT) program, 02-L493, sponsored by the Defense Advanced Research Projects Agency (DARPA). It was carried out under the auspices of the U.S. Department of Energy by the University of California, Lawrence Livermore National Laboratory under contract No. W-7405-Eng-48.

REFERENCES with titles

[1] John W. Hardy, *Adaptive Optics for Astronomical Telescopes*. (Oxford University Press, Oxford, 1998).

[2] R. K. Tyson, *Principles of Adaptive Optics*. (Academic Press, Boston, 1998).

[3] Charles A. Thompson, Michael W. Kartz, Laurence M. Flath, Scott C. Wilks, Richard A. Young, Gary W. Johnson and Anthony J. Ruggiero, “Free space optical communications utilizing MEMS adaptive optics correction,” in *Free-Space Laser Communication and Laser Imaging II*, Jennifer C. Ricklin and David G. Voelz, eds., Proc. SPIE **4821**, 129 (2002).

[4] David L. Fried, "Branch point problem in adaptive optics," J. Opt. Soc. Am. A **15** (10), 2759 (1998).

[5] Rensheng Dou and Michael K. Giles, "Closed-loop adaptive-optics system with a liquid-crystal television as a phase retarder," Opt. Lett. **20** (14), 1583 (1995).

[6] T. Shirai, T.H. Barnes and T.G. Haskell, "Adaptive wave-front correction by means of all-optical feedback interferometry," Opt. Lett. **25** (11), 773 (2000).

[7] K.L. Baker, E.A. Stappaerts, S.C. Wilks, P.E. Young, D. Gavel, J. Tucker, D.A. Silva and S.S. Olivier, "Open and Closed-Loop Aberration Correction using a Quadrature Interferometric Wave-Front Sensor," Opt. Lett. **29** (1), 47 (2004).

[8] Michael C. Roggeman, Victor M. Bright, Byron M. Welsh, Shaun R. Hick, Peter C. Roberts, William D. Cowan and John H. Comtois, “Use of micro-electro-mechanical deformable mirrors to control aberrations in optical systems: theoretical and experimental results,” Opt. Eng. **36** (5), 1326 (1997).

[9] K.L. Baker, E.A. Stappaerts, S.C. Wilks, D. Gavel, P.E. Young, J. Tucker, D.A. Silva, S.S. Olivier and J. Olsen, "Performance of a phase-conjugate-engine implementing a finite-bit phase correction," Opt. Lett. (2004).

[10] Thomas Weyrauch and Mikhail A. Vorontsov, “Mitigation of atmospheric-turbulence effects over 2.4-km near-horizontal propagation path with 134 control-channel MEMS/VLSI adaptive transceiver system,” in *Advanced Wavefront Control: Methods, Devices, and Applications*, John D. Gonglewski, Mikhail A. Vorontsov and Mark T. Gruneisen, eds., Proc. SPIE **5162**, 1 (2003).

[11] Thomas G. Bifano, Julie Perreault, Raji Krishnamoorthy Mali and Mark N. Horenstein, “Microelectromechanical Deformable Mirrors,” IEEE Journal of Selected Topics in Quantum Electronics **5** (1), 83 (1999).

[12] Thomas J. Flynn, "Two-dimensional phase unwrapping with minimum weighted discontinuity," JOSA A **14** (10), 2692 (1997).

[13] D.L. Fried, "Optical Resolution Through a Randomly Inhomogeneous Medium for Very Long and Very Short Exposures," J. Opt. Soc. Am. **56** (10), 1372 (1966).

[14] Gordon D. Love, Nigel Andrews, Philip Burch, David Buscher, Peter Doel, Colin Dunlop, John Major, Richard Myers, Alan Purvis, Ray Sharples, Andrew Vick, Andrew Zadrozny, Sergio R. Restaino and Andreas Glindemann, "Binary adaptive optics: atmospheric wave-front correction with a half-wave phase shifter," Applied Optics **34** (27), 6058 (1995).

REFERENCES without titles

[1] John W. Hardy, *Adaptive Optics for Astronomical Telescopes*. (Oxford University Press, Oxford, 1998).

[2] R. K. Tyson, *Principles of Adaptive Optics*. (Academic Press, Boston, 1998).

[3] Charles A. Thompson, Michael W. Kartz, Laurence M. Flath, Scott C. Wilks, Richard A. Young, Gary W. Johnson and Anthony J. Ruggiero, in *Free-Space Laser Communication and Laser Imaging II*, Jennifer C. Ricklin and David G. Voelz, eds., Proc. SPIE **4821**, 129 (2002).

[4] David L. Fried, J. Opt. Soc. Am. A **15** (10), 2759 (1998).

[5] Rensheng Dou and Michael K. Giles, Opt. Lett. **20** (14), 1583 (1995).

[6] T. Shirai, T.H. Barnes and T.G. Haskell, Opt. Lett. **25** (11), 773 (2000).

[7] K.L. Baker, E.A. Stappaerts, S.C. Wilks, P.E. Young, D. Gavel, J. Tucker, D.A. Silva and S.S. Olivier, Opt. Lett. **29** (1), 47 (2004).

[8] Michael C. Roggeman, Victor M. Bright, Byron M. Welsh, Shaun R. Hick, Peter C. Roberts, William D. Cowan and John H. Comtois, Opt. Eng. **36** (5), 1326 (1997).

[9] K.L. Baker, E.A. Stappaerts, S.C. Wilks, D. Gavel, P.E. Young, J. Tucker, D.A. Silva, S.S. Olivier and J. Olsen, Opt. Lett. (2004).

[10] Thomas Weyrauch and Mikhail A. Vorontsov, in *Advanced Wavefront Control: Methods, Devices, and Applications*, John D. Gonglewski, Mikhail A. Vorontsov and Mark T. Gruneisen, eds., Proc. SPIE **5162**, 1 (2003).

[11] Thomas G. Bifano, Julie Perreault, Raji Krishnamoorthy Mali and Mark N. Horenstein, IEEE Journal of Selected Topics in Quantum Electronics**5** (1), 83 (1999).

[12] Thomas J. Flynn, JOSA A **14** (10), 2692 (1997).

[13] D.L. Fried, J. Opt. Soc. Am. **56** (10), 1372 (1966).

[14] Gordon D. Love, Nigel Andrews, Philip Burch, David Buscher, Peter Doel, Colin Dunlop, John Major, Richard Myers, Alan Purvis, Ray Sharples, Andrew Vick, Andrew Zadrozny, Sergio R. Restaino and Andreas Glindemann, Applied Optics **34** (27), 6058 (1995).

FIGURE CAPTIONS

Figure 1 Field test setup used to test the performance of the phase conjugation engine over a 1.35 km atmospheric path. The abbreviations stand for the following: BS, beam splitters; M, mirrors; L, lenses; S, shutters; A, apertures; TFP, thin film polarizers; $\lambda/2$ and $\lambda/4$, half and quarter wave-plates, respectively.

Figure 2 Phase structure function averaged over 3000 measured functions, which were calculated by unwrapping the wrapped phases determined from 3000 sets of sine and cosine interferograms

Figure 3 Point-spread functions for the uncorrected and correct probe beams after propagation through the atmosphere.

Figure 4 Absolute Strehl ratios as a function of time. The solid black line represents the Strehl ratio with the AO system turned on, while the dashed black line represents the Strehl ratio with the system turned off. The solid gray line represents the Strehl ratio with the system turned off but with the center of mass of the point spread function moved to the central axis, as would occur if a tip/tilt system were running.

FIGURES

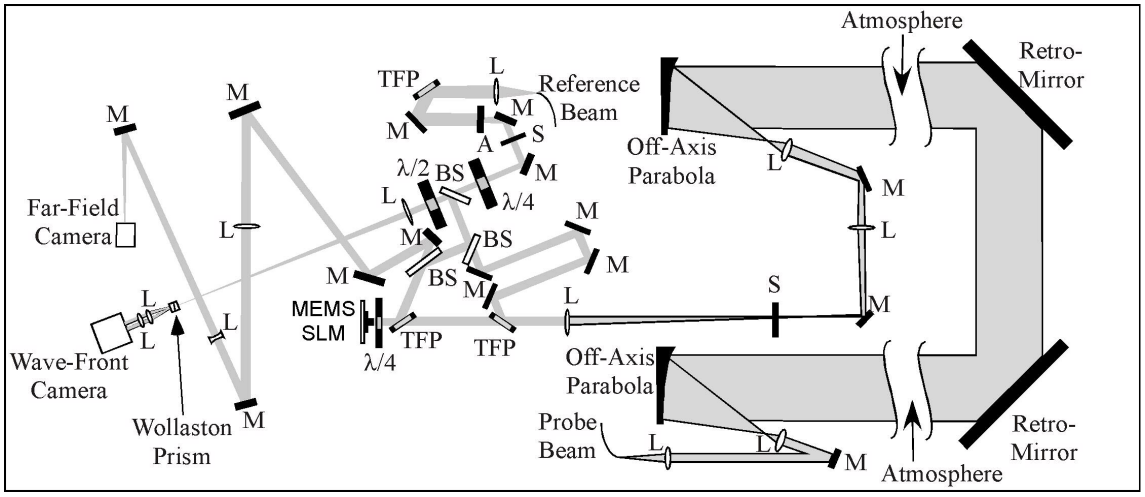

Figure 1

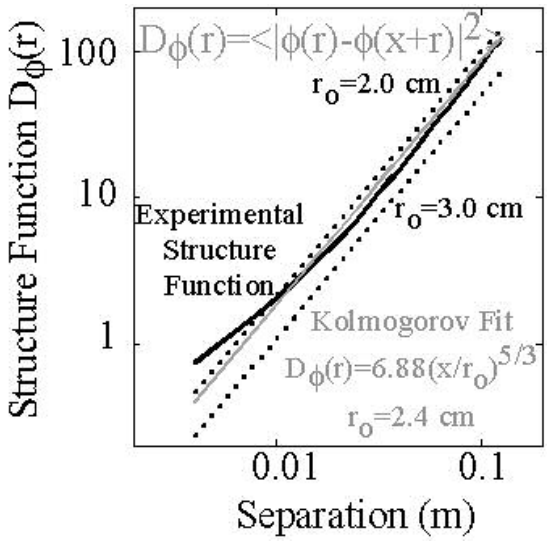
$D_\phi(r)=<|\phi(r)-\phi(x+r)|^2>$
r_o=2.0 cm
r_o=3.0 cm
Experimental
Structure
Function
Kolmogorov Fit
$D_\phi(r)=6.88(x/r_o)^{5/3}$
r_o=2.4 cm
Structure Function $D_\phi(r)$
100
10
1
0.01
0.1
Separation (m)

Figure 2

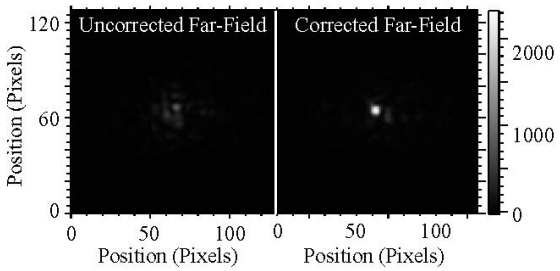
Uncorrected Far-Field
Corrected Far-Field
Position (Pixels)
Position (Pixels)
Position (Pixels)
120
60
0
0
50
100
0
50
100
2000
1000
0

Figure 3

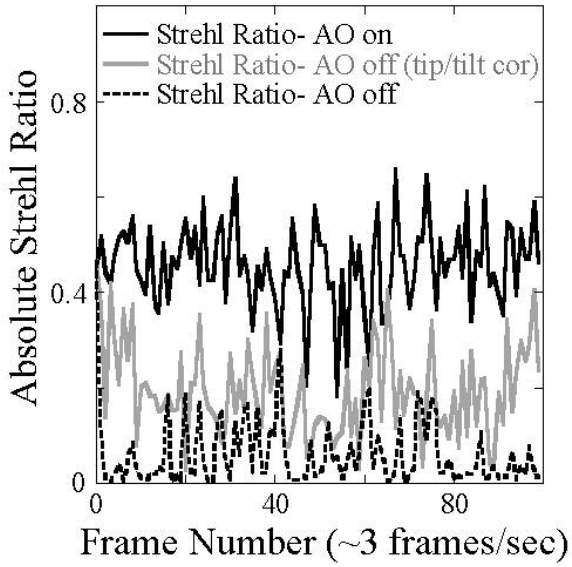
Strehl Ratio- AO on
Strehl Ratio- AO off (tip/tilt cor)
Strehl Ratio- AO off
Absolute Strehl Ratio
0.8
0.4
0
0
40
80
Frame Number (~3 frames/sec)

Figure 4

University of California
Lawrence Livermore National Laboratory
Technical Information Department
Livermore, CA 94551